

## AIRCRAFT & CAR SHAPE OPTIMIZATION ON THE RBF4AERO PLATFORM

D.H. Kapsoulis<sup>1</sup>, V.G. Asouti<sup>1</sup>, E.M. Papoutsis-Kiachagias<sup>1</sup>, K.C. Giannakoglou<sup>1</sup>,  
S. Porziani<sup>2</sup>, E. Costa<sup>2</sup>, C. Groth<sup>3</sup>, U. Cella<sup>3</sup>, M. E. Biancolini<sup>3</sup>, M. Andrejašić<sup>4</sup>, D. Eržen<sup>4</sup>, M.  
Bernaščić<sup>5</sup>, A. Sabellico<sup>5</sup> and G. Urso<sup>5</sup>

<sup>1</sup>Parallel CFD & Optimization Unit, School of Mech. Eng.,  
National Technical University of Athens, Athens, Greece

e-mail: jim.kapsoulis@gmail.com, vasouti@mail.ntua.gr, [vaggelisp@gmail.com](mailto:vaggelisp@gmail.com), [kgianna@central.ntua.gr](mailto:kgianna@central.ntua.gr)

<sup>2</sup>D'Appolonia S.p.A.  
Viale Cesare Pavese 305, 00144 Rome, Italy  
e-mail: {stefano.porziani, [emiliano.costa}@dappolonia.it](mailto:emiliano.costa}@dappolonia.it)

<sup>3</sup>Dept. of Enterprise Engineering  
University of Rome Tor Vergata, Via Politecnico 1, 00133, Rome Italy  
e-mail: [biancolini@ing.uniroma2.it](mailto:biancolini@ing.uniroma2.it)

<sup>4</sup>Dept. of Aerodynamics  
PIPISTREL d.o.o. Ajdovščina, R&D, Slovenia  
e-mail: matej.andrejasic@pipistrel.si, [david@pipistrel.si](mailto:david@pipistrel.si)

<sup>5</sup>Institute of Applied Computing  
National Research Council of Italy, Via dei Taurini, 19, 00185 Rome Italy  
e-mail: {m.bernaščić, a.sabellico, g.urso}@iac.cnr.it

**Keywords:** Shape Optimization, Metamodel, Evolutionary Algorithms, Continuous Adjoint, RBF Morphing.

### ABSTRACT

*This paper demonstrates the solution of industrial aerodynamic shape optimization problems using the optimization methods provided by the RBF4AERO platform, developed in the framework of the EU-funded RBF4AERO project (Grant Agreement No: 605396). The platform provides a complete infrastructure needed for optimization problems, including GUI, Optimization Algorithms, CFD Solvers, Morpher Tool and Benchmark Management System. Both stochastic and gradient-based optimization methods are implemented on this platform. The design variables are related to a morphing tool based on Radial Basis Functions (RBFs) which control the deformation of both surface and volume meshes. Whenever the optimization is based on gradient-based techniques, the continuous adjoint method is used to compute the sensitivity derivatives while the Morpher tools give the mesh deformation velocity. The stochastic tool is based on Evolutionary Algorithms (EAs) assisted by surrogate evaluation models (Response Surface Methods, RSM). A sampling technique (Design of Experiments) provides the training patterns of the RSM which is exclusively used as the evaluation tool within the EA-based optimization. At the end of each EA-based optimization, the resulting “optimal” solution(s) are re-evaluated by means of the CFD tool, before proceeding to the next cycle if needed. The optimization of car and aircraft models on the RBF4AERO platform is showcased.*

### 1 INTRODUCTION

Aerodynamic shape optimization is an attractive topic for both academia and industries. An automated shape optimization loop includes the shape parameterization scheme (the parameters of which act as the design variables), the flow (CFD) solver, an optimization method capable of computing the optimal value set of the design variables and a method adapting (or regenerating) the CFD mesh to each candidate solution.

Optimization methods can be classified into two main categories, stochastic and gradient-based ones. The most widely used stochastic methods are the Evolutionary Algorithms (EAs) which, apart from their flexibility, may compute the global optimum, though at a computational cost that scales with the number of design

variables. For this reason, the use of "standard" EAs in large scale optimization problems becomes often prohibitively expensive. A remedy to this problem is the implementation of surrogate evaluation models or metamodels, leading to the so-called metamodel-assisted EAs (MAEAs). Their role is to replace the exact evaluation tool (CFD code), thus reducing the total number of expensive evaluations required to reach the optimal solution(s). MAEAs could be based on on-line trained metamodels, such as artificial neural networks or RSM, that are trained on the fly during the evolution, based on the already evaluated individuals, as in [1]. The RBF4AERO platform, though, supports off-line trained metamodels. In fact, there is a single global metamodel built which needs a sampling technique, often referred to as Design of Experiments (DoE), [2], to collect the necessary training patterns. The trained metamodel is used as the evaluation tool during the EA-based search.

In aerodynamic shape optimization, gradient-based methods mostly rely upon the (discrete or continuous) adjoint method [3] to compute the gradient of the objective function; they require a greater effort for development and code maintenance whereas new method developments are due if a new flow model or objective function is to be used; in return, the cost per optimization cycle does not scale with the number of design variables. In this work, a continuous adjoint method [4] (first-differentiate-then-discretize; implemented on an in-house version of the OpenFOAM software, <http://www.openfoam.com>) that also differentiates the turbulence model is used to compute the sensitivities of the drag (objective function) w.r.t. the shape controlling parameters.

Either with stochastic or gradient-based optimization methods, a shape/mesh morphing tool may help a lot to avoid repetitive costly re-meshing tasks since it simultaneously affects the surface to be designed and the CFD mesh. Radial Basis Functions (RBFs, [6]), volumetric B-splines or NURBS [5] etc can be used as morphing tools. Here, the RBF Morph software [6], is employed. Parameters controlling the positions of groups of RBF control points are used as design variables.

This paper presents the use of the above-mentioned optimization methods on the RBF4AERO platform. This platform is developed to support top-level aeronautical designs, including multi-physics and multi-objective optimization, fluid-structure interaction and ice accretion simulation. The use of the RBF mesh morphing technique significantly boosts the aerodynamic design process. EAs and adjoint methods are included. Applications on a car and an ultra-light aircraft shape optimization problem are presented.

## 2 EA-based Optimization using Metamodels

The EA-based optimization algorithm integrated within the RBF4AERO platform implements metamodels to reduce the CPU cost. First thing is the definition of the design variables. Once the shape is controlled by the morphing tool, the latter provides the  $N$  design variables. A DoE technique selects individuals to undergo evaluation on the CFD tool, after appropriately deforming the baseline mesh using RBF Morph. The evaluated individuals (design variable value sets paired with the corresponding performance metric computed by a CFD code) are stored in the database (DB) and become the training patterns for the RSM. An EA-based optimization runs by performing evaluations on the trained RSM and converges to the "optimal" solution(s); quotes are used since the evaluation is based on the metamodel. "Optimal" solution(s) need to be evaluated anew on the CFD code and appended to the DB. Depending on the gap between CFD and metamodel-based predictions, the RSM might be trained anew before starting a new optimization cycle. The RSM training, the EA-based optimization and the re-evaluation(s) constitute the three phases of an optimization cycle. If a subset of the design space is not explored sufficiently, there is an option to continue with additional CFD evaluations. All the optimization algorithm settings, i.e. the DoE, the RSM and the EA parameters are user-defined through the RBF4AERO platform GUI. The overall optimization process is shown in fig. 1.

The individuals selected by the DoE are evaluated and used to train the metamodel. The RBF4AERO platform implements a regression model (RSM) [7] based on polynomial functions,

$$\hat{F}(\vec{x}) = b_0 + \sum_{i=1}^N \sum_{j=1}^{P_i} b_{ij} x_i^j + \sum_{j=0}^M a_j \prod_{i=1}^N x_i^{l_i} \quad (1)$$

where  $\hat{F}$  is the approximate objective function value,  $x_i$  is the  $i^{th}$  design variable,  $M$  the number of interactions,  $l_i$  the power that design variable  $i$  is raised to and  $P_i$  the maximum power for each variable. The training phase computes the RSM's coefficients  $b_{ij}, a_j$ . Interactions, [8], are factors which multiply the design variables with each other. These factors are replicating the relationship and the dependence between the design variables. The least-squares method is used to train the RSM, because the number of training patterns may exceed the number of the coefficients to be computed. The training cost depends on the number of unknown coefficients. The  $P_i$  and  $l_i$  values of eq.1 can be either selected by the user or automatically defined by minimizing the RSM's error. A different RSM, i.e. with different configuration (maximum powers, interactions), is trained for each objective function and constraint of the problem.

After having trained the metamodel, a  $(\mu, \lambda)$  EA, with  $\mu$  parents and  $\lambda$  offspring, undertakes the optimization by exclusively evaluating offspring on the RSM tool. A real-coded EA with tournament selection

for the parent population and a simulated binary crossover scheme is implemented. The computational cost of RSM is negligible. Upon the termination of the evolution, the “optimal” solution(s) resulting from EA are re-evaluated on the CFD tool and added to the DB.

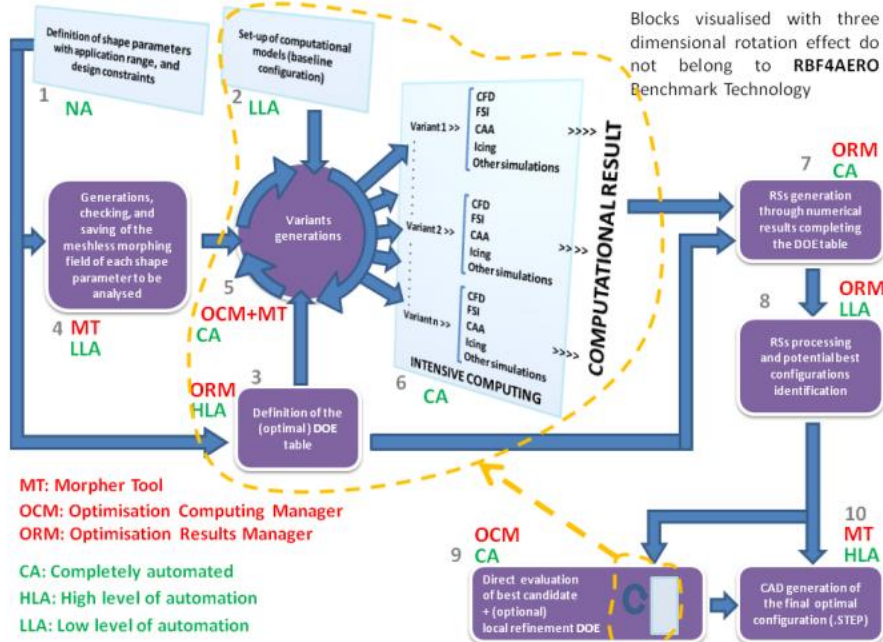


Figure 1. The RBF4AERO optimization platform.

The optimization loop terminates if any of the following three criteria is met. The first criterion is related to the computational budget and is quantified by the maximum number of CFD evaluations the user may afford. This limits the size of the initial sampling and the times RSM can be re-trained. The second criterion is related to the RSM prediction accuracy; we consider that the optimal solutions have been found, if the RSM error is very small and its prediction practically replicates the objective function value which results from the CFD tool. The third criterion stops the EA if the “optimal” solution does not improve during a number of evaluations.

### 3 The Continuous Adjoint Method

In this section, the formulation of the continuous adjoint PDEs to the incompressible Navier-Stokes equations, their boundary conditions and the sensitivity derivatives (gradient) expression are presented in brief. The mean flow equations together with the Spalart-Allmaras turbulence model PDE, [9],

$$\begin{aligned}
 R^P &= -\frac{\partial v_i}{\partial x_i} = 0 \\
 R^v_j &= v_j \frac{\partial v_i}{\partial x_j} - \frac{\partial \tau_{ij}}{\partial x_j} + \frac{\partial p}{\partial x_i} = 0 \\
 R^{\bar{v}}_j &= -\frac{\partial(v_j \tilde{v})}{\partial x_j} - \frac{\partial}{\partial x_j} \left[ \left( v + \frac{\tilde{v}}{\sigma} \right) \frac{\partial \tilde{v}}{\partial x_j} \right] - \frac{c_{b2}}{\sigma} \left( \frac{\partial \tilde{v}}{\partial x_j} \right)^2 - \tilde{v} (P(\tilde{v}, \Delta) - D(\tilde{v}, \Delta)) = 0
 \end{aligned} \tag{2}$$

comprise the flow or primal system of equations, where  $\tau_{ij} = (v + v_t) \left( \frac{\partial v_i}{\partial x_j} + \frac{\partial v_j}{\partial x_i} \right)$  are the components of the stress tensor,  $v_i$  are the velocity components,  $p$  is the static pressure divided by the density,  $v$  and  $v_t$  the bulk and turbulent viscosities, respectively,  $\tilde{v}$  the Spalart-Allmaras model variable and  $\Delta$  the distance from the wall boundaries.

Let  $F$  be the objective function to be minimized by computing the optimal values of the design variables  $b_n, n \in [1, N]$ . A general expression for  $F$  defined on (parts of) the boundary  $S$  of the domain  $\Omega$  is

$$F = \int_S F_{S_i} n_i dS \tag{3}$$

where  $\mathbf{n}$  is the outward normal unit vector. Differentiating eq.3 w.r.t to  $b_n$  and applying the chain rule yields

$$\begin{aligned} \frac{\delta F}{\delta b_n} = & \int_S \frac{\partial F_{S_i}}{\partial v_k} n_i \frac{\partial v_k}{\partial b_n} dS + \int_S \frac{\partial F_{S_i}}{\partial p} n_i \frac{\partial p}{\partial b_n} dS + \int_S \frac{\partial F_{S_i}}{\partial \tau_{kj}} n_i \frac{\partial \tau_{kj}}{\partial b_n} dS + \int_S \frac{\partial F_{S_i}}{\partial \tilde{v}} n_i \frac{\partial \tilde{v}}{\partial b_n} dS + \\ & \int_S n_i \frac{\partial F_{S_i}}{\partial x_k} \frac{\delta x_k}{\delta b_n} n_k dS + \int_S F_{S_i} \frac{\delta(n_i dS)}{\delta b_n} \end{aligned} \quad (4)$$

where  $\frac{\delta \Phi}{\delta b_n}$  denotes the total derivative of any quantity  $\Phi$  while  $\frac{\partial \Phi}{\partial b_n}$  is its partial derivative.

The continuous adjoint formulation starts from the definition of the augmented objective function

$$F_{\text{aug}} = F + \int_{\Omega} u_i R_i^V d\Omega + \int_{\Omega} q R^P d\Omega + \int_{\Omega} \tilde{v}_a R^{\bar{V}} d\Omega \quad (5)$$

where  $u_i$  are the components of the adjoint velocity vector,  $q$  is the adjoint pressure and  $\tilde{v}_a$  is the adjoint turbulence model variable, respectively. The Spalart-Allmaras model PDE has been differentiated as in [10]. The differentiation of eq.5, based on the Leibniz theorem, yields

$$\frac{\delta F_{\text{aug}}}{\delta b_n} = \frac{\delta F}{\delta b_n} + \int_{\Omega} u_i \frac{\partial R_i^V}{\partial b_n} d\Omega + \int_{\Omega} q \frac{\partial R^P}{\partial b_n} d\Omega + \int_{\Omega} R^{\bar{V}} \frac{\partial R^{\bar{V}a}}{\partial b_n} d\Omega + \int_{S_W} (u_i R_i^V + q R^P + \tilde{v}_a R^{\bar{V}}) n_k \frac{\partial x_k}{\partial b_n} dS \quad (6)$$

Then, the derivatives of the flow residuals in the volume integrals of eq.6 are developed by differentiating eq.2 and applying the Green-Gauss theorem. This development can be found in [10] and [11].

In order to obtain a gradient expression free of partial derivatives of the flow variables w.r.t.  $b_n$ , their multipliers in (the developed form of) eq.6 are set to zero, by satisfying the field adjoint equations

$$\begin{aligned} R^q &= -\frac{\partial u_j}{\partial x_j} = 0 \\ R_i^V &= u_j \frac{\partial v_j}{\partial x_i} - \frac{\partial(v_j u_i)}{\partial x_j} - \frac{\partial \tau_{ij}^a}{\partial x_j} + \frac{\partial q}{\partial x_i} - \tilde{v}_\alpha \frac{\partial \tilde{v}}{\partial x_i} - \frac{\partial}{\partial x_i} \left( \tilde{v}_a \tilde{v} \frac{C_Y}{Y} e_{mjk} \frac{\partial v_k}{\partial x_j} e_{mli} \right) = 0 \quad (b) \\ R^{\bar{V}\alpha} &= -\frac{\partial(v_j \tilde{v}_\alpha)}{\partial x_j} - \frac{\partial}{\partial x_j} \left[ \left( v + \frac{\tilde{v}}{\sigma} \right) \frac{\partial \tilde{v}_\alpha}{\partial x_j} \right] + \frac{1}{\sigma} \frac{\partial \tilde{v}_\alpha}{\partial x_j} \frac{\partial \tilde{v}}{\partial x_j} + 2 \frac{c_{b2}}{\sigma} \frac{\partial y}{\partial x_j} \left( \tilde{v}_\alpha \frac{\partial \tilde{v}}{\partial x_j} \right) + \tilde{v}_\alpha \tilde{v} C_{\bar{V}} \\ &+ \frac{\partial v_t}{\partial \tilde{v}} \frac{\partial u_i}{\partial x_j} \left( \frac{\partial v_i}{\partial x_j} + \frac{\partial v_j}{\partial x_i} \right) + (D - P) \tilde{v}_\alpha = 0 \end{aligned} \quad (7)$$

where  $\tau_{ij}^a = (v + v_t) \left( \frac{\partial u_i}{\partial x_j} + \frac{\partial u_j}{\partial x_i} \right)$  are the components of the adjoint stress tensor. The last equation is the adjoint turbulence model one, from which the adjoint turbulence model variable  $\tilde{v}_\alpha$  is computed. The adjoint boundary conditions are derived by treating the flow variations in the boundary integrals of eq.6. This development and the remaining terms which give the sensitivity derivatives are presented in detail in [10], [11].

The gradient-based algorithm used to minimize the objective function is described in brief below:

1. Define the shape modification parameters (design variables,  $b_i$ ).
2. Solve the flow equations (eqs.2).
3. Compute the drag force value,  $F_D = \int_{S_W} (-\tau_{ij} + p \delta_i^j) n_j r_i dS$ , where  $\vec{r}$  is a unit vector parallel to the farfield velocity.
4. Solve the adjoint equations, eqs. 7.
5. Compute the deformation velocities and through them, the sensitivity derivatives.
6. Update the design variables by  $\Delta b_i = -\eta \delta F / \delta b_i$ , where  $\eta$  is a user-defined step.
7. Update the surface and the CFD mesh through the morphing tool.
8. Unless the stopping criterion is met, go to step 2.

#### 4 RBF-Based Morphing

The individuals determined by the DoE or the adjoint method are evaluated on the CFD tool. In this paper, all evaluations are carried out using the steady state solver of OpenFOAM. For each candidate solution, a new mesh is adapted to the new geometry. Instead of re-meshing, an RBF-based morpher undertakes the modification of a baseline mesh before delivering it to the evaluation manager for the CFD run. All baseline meshes have been generated using the snappyHexMesh tool of OpenFOAM.

RBFs are mathematical functions able to interpolate data defined at discrete points only (source points) in an n-dimensional environment. The RBF expression has the following form:

$$s(x) = \sum_{i=1}^N \gamma_i \varphi(||x - x_{k_i}||) + h(x) \quad (8)$$

where  $\gamma$  and the coefficients of the polynomial  $h(x)$  are fitted by imposing the known values at source points  $x_{k_i}$ .  $\varphi$  controls the quality and behavior of the interpolation. The bi-harmonic function  $\phi(r) = r$  is well established, smooth and fast, that is why this is used in 3D mesh morphing. A linear system with size equal to the number of considered source points (RBF centers) is solved to compute the coefficients. The displacement of any mesh node can be computed as a function of the distance-based contributions from each RBF center.

The RBF method has some attractive advantages for mesh morphing. First of all, it is amenable to parallelization, because the displacement of each node does not depend on connectivity data. Additionally, it is able to exactly prescribe known deformations onto the surface mesh. This can be achieved by using all the mesh nodes as RBF centers with prescribed displacements, where a surface which is left untouched takes on zero displacements. The RBF Morph software [6], included in the RBF4AERO platform, has a fast solver capable to fit large dataset (hundreds of thousands of RBF points can be fitted in a few minutes) and with a suite of modeling tools that allows the user to easily set-up each shape modification. So, this software is able to cope with the challenges raised from industrial mesh morphing applications.

## 5 Application I: Optimization of the DrivAer car model

In this section, the two optimization algorithms (EA and adjoint based) are utilized to minimize the drag force exerted on the surface of the DrivAer car model; this is a generic car model developed at the Institute of Aerodynamics and Fluid Mechanics of TU Munchen, [12], to facilitate aerodynamic investigations of passenger cars. The fast-back DrivAer configuration with smooth underbody, with mirrors and wheels (F\_S\_wm\_ww) is used here. Six shape deformation variables (design variables) are defined in total and the corresponding deformation velocities are depicted in fig. 2.

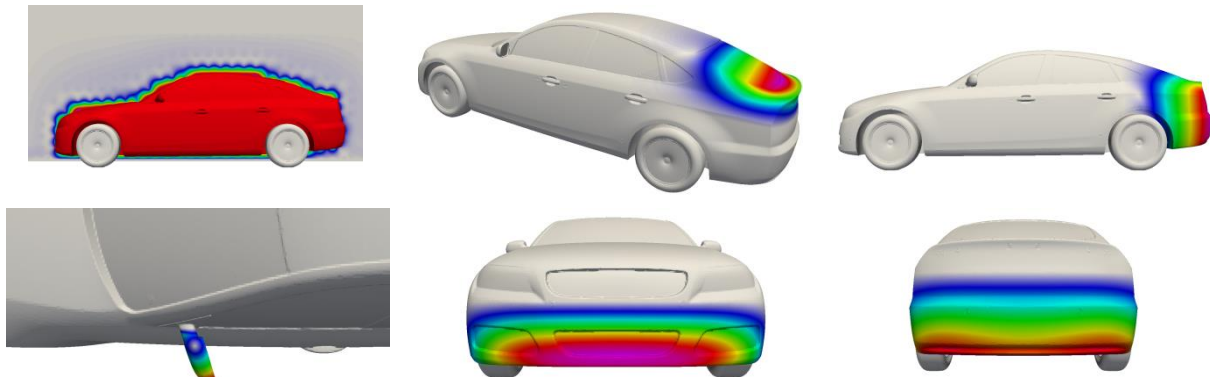


Figure 2. DrivAer Shape Optimization: Deformation velocities on the car surface, corresponding to the normal displacement of the surface caused by a "unit" displacement of the six design variables, according to the morphing tool set-up.

A computational mesh of approximately 5 million cells is used and turbulence is modeled by means of the Spalart–Allmaras model with wall functions. In the sake of simplicity, the steady state solver (simpleFOAM) was used even though the flow around the car varies in time. 15 optimizations cycles were needed by the adjoint-based method to reduce the mean drag value by more than 7%. The evolution of the objective function value during the flow solver iterations over the optimization cycles is shown in fig. 3 (left).

The same case was also optimized with EAs. A random factorial design selected 20 samples at the 0<sup>th</sup> optimization cycle and, based on them, the RSM was trained. A (25, 50) EA with max 500 evaluations on the RSM follows and its “optimal” solution was re-evaluated on the CFD tool and the result was recorded in the DB. 10 optimization cycles in total were necessary for the optimization to convergence, see fig. 3 (right).

Both methods yield almost similar results, more or less at the same computational cost and both reduce the objective function value by about 7%. The resulting optimal geometries are similar and small differences can be identified in the front bumper and the spoiler, see fig. 4. The pressure fields, plotted over the initial and optimized geometries that resulted from the EA-based optimization are shown in fig. 5 and 6.

The area with the highest deformation is located at the rear part of the car. The first major displacement is associated with reshaping the rear windshield by lowering its height and also a spoiler is formed at the end of the trunk. This creates an area of increased pressure at the bottom of the rear windshield and despite the increased pressure on top of the formed spoiler, a force pushing the car forward is generated. The second trend is to create a “boat tail” effect which increases the pressure at the rear side of the car, contributing thus to drag reduction.

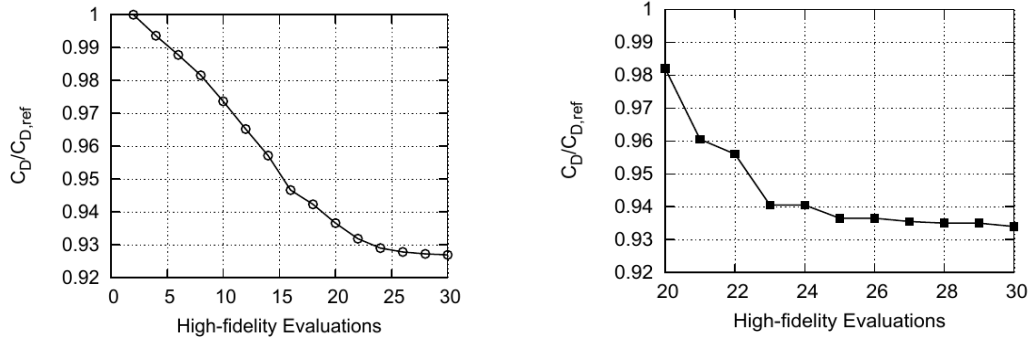


Figure 3. DrivAer Shape Optimization: Convergence histories of the adjointt-based optimization (left) and the EA (right).

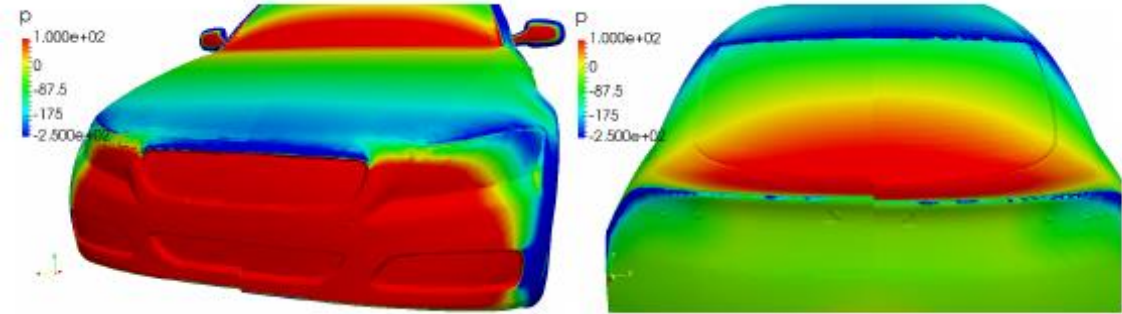


Figure 4. DrivAer Shape Optimization: Comparison between the "optimal" shapes computed by the EA- (starboard) and the adjoint-based (port) optimization

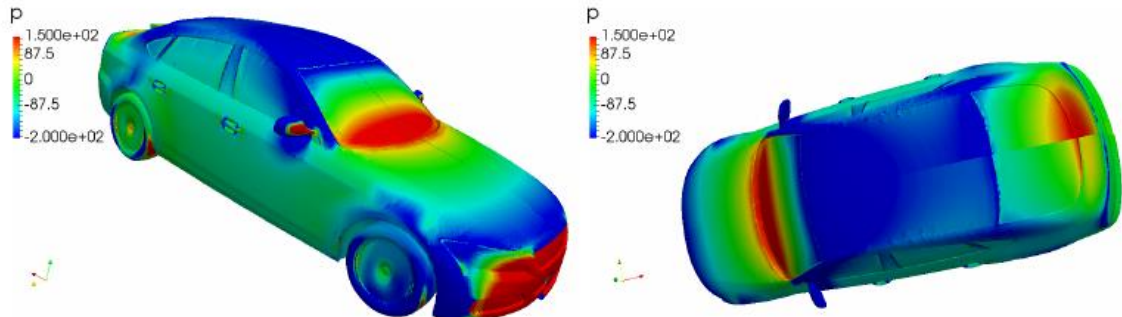


Figure 5. DrivAer Shape Optimization: Shape comparison between the baseline (port) and "optimal" shapes (starboard). Isobar contours are plotted.

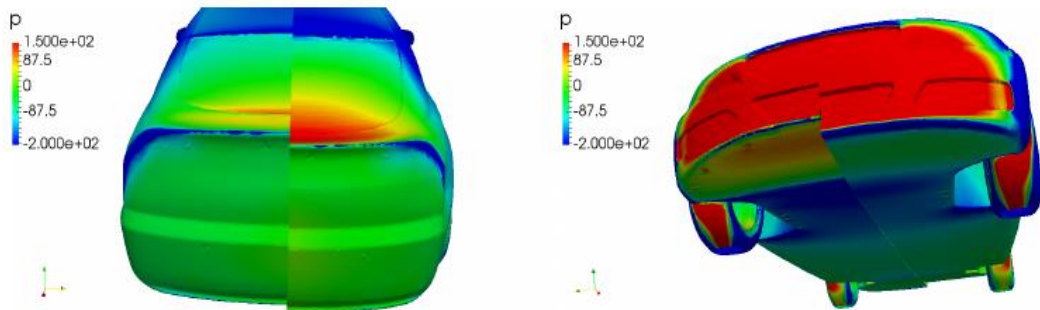


Figure 6. DrivAer Shape Optimization: Comparison between baseline (port) and "optimal" shapes (starboard).

## 6. Application II: Optimization of an Ultra-Light Aircraft

The second case is concerned with the re-design/optimization of an ultra-light aircraft [13]. The aircraft (reference) geometry was provided by Pipistrel, a light aircraft manufacturer partner of the RBF4AERO project. The flow conditions are  $M_\infty = 0.08$ ,  $\alpha_\infty = 10^\circ$  and  $Re = 10^6$  (based on the wing chord). Each candidate solution is evaluated on simpleFoam coupled with the Spalart-Allmaras turbulence model with wall functions. The CFD mesh around the reference aircraft is unstructured with approximately 4.7M cells.

An optimization is performed with the EA method aiming at the minimization of its drag coefficient. The re-design focuses on the wing root-body junction by defining two boxes, the larger one for restricting the morphing action and smaller one that contains the entire wing. The second box acts via 3 design variables; these correspond to the displacements of the control box in the x, y, z axes. The RBF Morpher deforms the CFD mesh outside the small box while keeping the mesh around the big box intact. The 45 samples, selected by a random design and evaluated on the CFD tool, are used to train the 6<sup>th</sup> degree ( $P_i = 6$ ) RSM. Then a (15, 30) EA undertakes the optimization with a termination criterion of 500 evaluations on the RSM and its “optimal” solution is re-evaluated on the CFD tool. The DB is enriched and the RSM is re-trained. Note that each time the RSM should be retrained, a different degree and coefficients of the RSM’s equation might be used. 10 optimization cycles were performed. The convergence history of the optimization, without including the initial DoE samples’ evaluations, is shown in fig. 7.

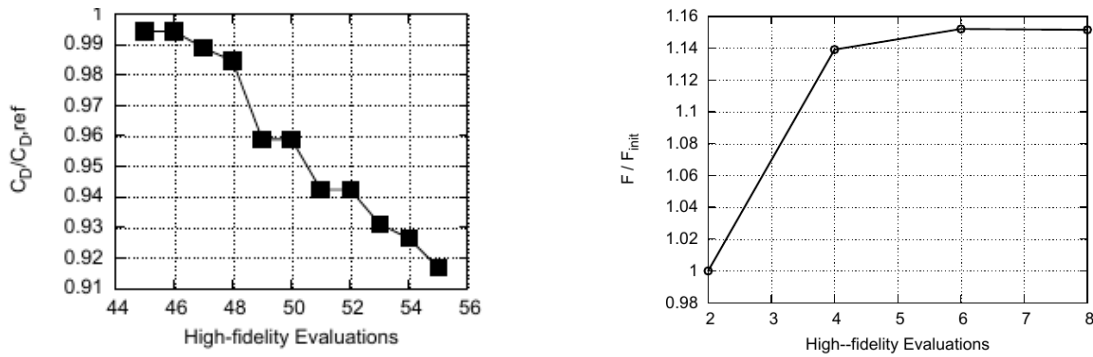


Figure 7. Ultra-light Aircraft Shape Optimization: Convergence history of the EA-based (left) and the adjoint-based (right) optimization.

Compared to the reference aircraft, the optimization has reduced the drag coefficient by 9%, due to the displacement of the junction towards the rear and bottom part of the fuselage. A by-product of the optimization is that the lift has increased, even though this has not been included in the objective function. A comparison of the pressure field on the aircraft surface, between the reference and the “optimal” shape, is shown in fig. 8.

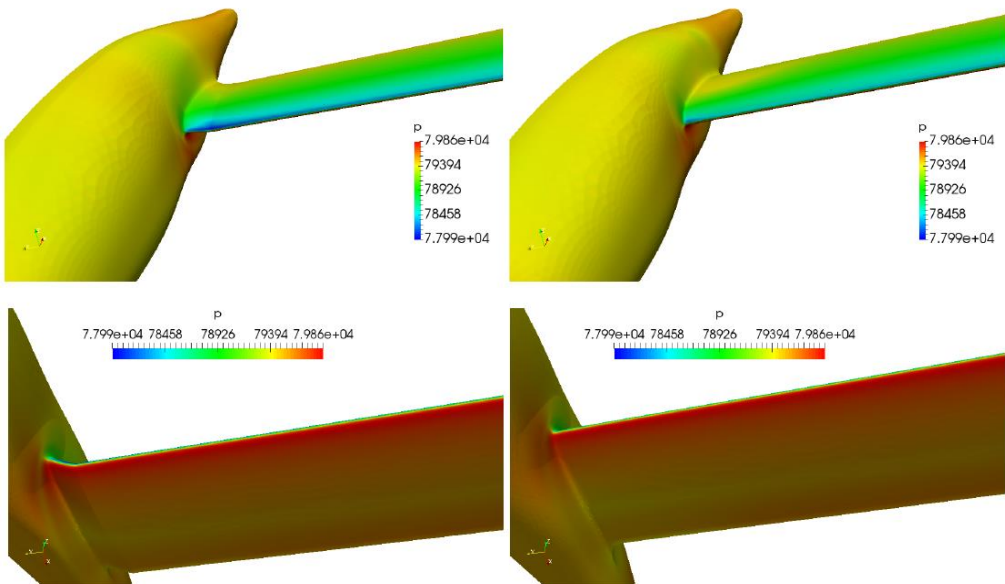


Figure 8. Ultra-light Aircraft Shape Optimization: Comparison of the reference (right) and the “optimal” (left) shape from the front (top) and bottom (bottom) view.

The adjoint-based method performed a slightly different optimization on the same aircraft by trying to maximize the lift-to-drag ratio. The geometry is controlled by four RBF-based design variables which may change the shape of the wing-fuselage junction close to the leading and trailing edges as well as parts of the upper fuselage surface. The convergence of the optimization algorithm is shown in fig 9. It can be observed that the lift-to-drag ratio has increased by 15%, caused by 10% drag reduction and a 4% lift increase. The optimized geometry is illustrated in fig. 9.

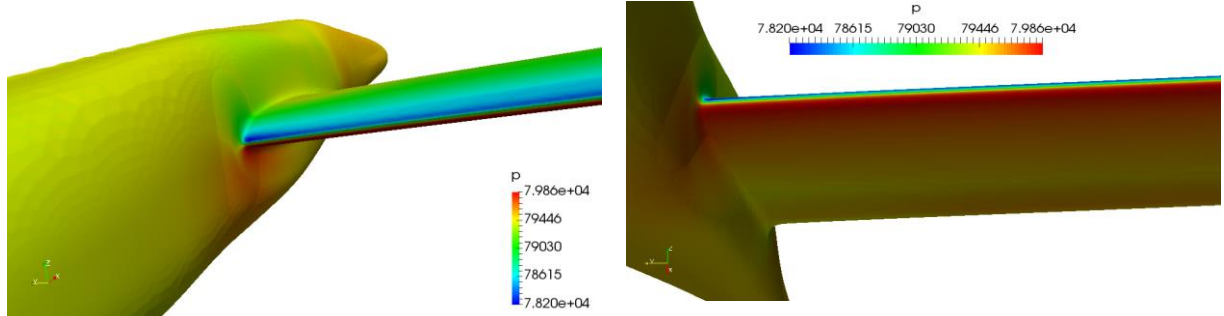


Figure 9. Ultra-light Aircraft Shape Optimization: Optimal solution's shape obtained using the gradient-based optimization.

## 6. Conclusions

In this paper, a demonstration of the RBF4AERO benchmark technology platform and its optimization capabilities were attempted. The platform aims to run/solve optimization problems in less computational cost in contrast with current practices and with flexibility for the user. Under the same platform, EA or adjoint-based optimization software combined with the RBF Morpher tool and CFD/FEM solvers form two optimization strategies which achieve the aforementioned goal. These methods were applied for the optimization of two industrial cases, a car model and an ultra-light aircraft.

---

**REFERENCES**

- [1] K.C. Giannakoglou (2002). Design of optimal aerodynamic shapes using stochastic optimization methods and computational intelligence', International Review Journal Progress in Aerospace Sciences, (38):43-76.
- [2] D.C. Montgomery (2008). Design and analysis of experiments. 5<sup>th</sup> edition.
- [3] M. Giles and N. Pierce (2000). An introduction to the adjoint approach to design. Flow, Turbulence and Combustion, (65):393–415.
- [4] S. Nadarajah and A. Jameson (2001). Studies of the continuous and discrete adjoint approaches to viscous automatic aerodynamic shape optimization. 15<sup>th</sup> Computational Fluid Dynamics Conference, Anaheim, CA, AIAA: 2001-2530.
- [5] M.J. Martin, E. Andres, C. Lozano, and E. Valero (2014). Volumetric b-splines shape parametrization for aerodynamic shape design. Aerospace Science and Technology, (37):26–36.
- [6] M.E. Biancolini (2014). Mesh morphing and smoothing by means of radial basis functions (RBF): A practical example using fluent and RBF morph. Handbook of Research on Computational Science and Engineering, Ch. 15 :347-380.
- [7] D.C. Montgomery and R. Myers (2002). Response surface methodology process and product optimization using designed experiments. 2<sup>nd</sup> edition.
- [8] J. F. Kenney and E.S. Keeping (1962). Linear regression and correlation. Mathematics of Statistics, 3<sup>rd</sup> edition, Ch. 15.
- [9] P. Spalart and S. Allmaras (1992). A one-equation turbulence model for aerodynamic flows. AIAA 30<sup>th</sup> Aerospace Sciences Meeting and Exhibit, Reno, Nevada.
- [10] A. Zymaris, D. Papadimitriou, K. Giannakoglou and C. Othmer (2009). Continuous adjoint approach to the Spalart-Allmaras turbulence model for incompressible flows. Computers & Fluids (38):1528–1538.
- [11] E. Papoutsis-Kiachagias and K. Giannakoglou (2014). Continuous adjoint methods for turbulent flows, applied to shape and topology optimization: Industrial applications. Archives of Computational Methods in Engineering DOI:10.1007/s11831-014-9141-9.
- [12] A. Heft, T. Indinger, and N. Adams (2012). Experimental and numerical investigation of the DrivAer model. ASME, Symposium on Issues and Perspectives in Automotive Flows.
- [13] M.E. Biancolini, E. Costa, U. Cellia, C. Groth, G. Veble, and M. Andrejasic (2016). Glider fuselage-wing junction optimization using CFD and RBF mesh morphing. Aircraft Engineering and Aerospace Technology, DOI: 10.1108/AEAT-12-2014-0211.R1.